

## Dual detection of COVID-19 antigens and antibodies using nanoscale fluorescent plasmonic substrates

Benjamin Taubner, Ashley Gibbons and Nathaniel C Cady 

College of Nanoscale Science & Engineering, SUNY Polytechnic Institute, Albany, NY 12203, USA  
Corresponding author: Nathaniel C Cady. Email: cadyn@sunypoly.edu

### Impact Statement

The COVID-19 pandemic has illustrated the need for rapid and accurate biosensors that can diagnose disease and assess immune responses to disease or vaccination. In this study, we demonstrated the potential to perform SARS-CoV-2 antigen detection for direct diagnosis of COVID-19 infection paired with a SARS-CoV-2 antibody test which was previously shown to have high diagnostic power for past COVID-19 infection and immune response to vaccination. The entire assay can be conducted in 1 h, making it useful for rapid diagnostics with quick results. While the core technology, GC-FP, has been previously demonstrated for antibody detection, it has never been demonstrated for direct antigen detection with paired capture/detection antibodies. Furthermore, to our knowledge, this is the first demonstration of co-detection of SARS-CoV-2 antibodies and antigens on a single biosensor chip or consumable. Therefore, this represents a potentially new paradigm for co-detection that will simplify the overall diagnostic process and provide additional clinical information in a single test.

### Abstract

There is a continuing need for biosensors that can be used in the diagnosis of COVID-19 infection and to measure a subject's immune response to the virus itself (SARS-CoV-2). In this study, grating-coupled fluorescent plasmonic (GC-FP)-based detection of SARS-CoV-2 antigens was coupled with antibody detection to yield a dual-mode detection assay. Pairs of capture and detection antibodies were screened for direct detection of the SARS-CoV-2 nucleocapsid (Nuc) antigen, which were then combined with an existing GC-FP antibody detection assay. Nuc could be detected as low as 1  $\mu\text{g/mL}$  concentrations, while antibodies were detectable to 50 ng/mL. The dual detection assay was tested by adding purified Nuc antigen to serum from a polymerase chain reaction (PCR)-positive COVID-19-infected individual. Using this sample, co-detection of Nuc antigen and anti-spike protein antibodies was successfully performed on a single GC-FP chip. Total assay time was 1 h, making this the first known example of rapid dual antibody and antigen detection on the same biosensor chip.

**Keywords:** Biosensor, COVID-19, antibody, antigen, plasmonic

**Experimental Biology and Medicine 2022; 247: 2081–2089. DOI: 10.1177/15353702221113860**

### Introduction

The COVID-19 pandemic, caused by the SARS-CoV-2 virus, has highlighted the need for rapid and accurate diagnostic tools that can be used for direct detection of viral pathogens, in addition to serological detection of antibodies generated through infection or vaccination. In previous work, we demonstrated that nanoscale surface plasmon resonance gratings can be used in fluorescence enhancement mode for the detection of antibodies produced in human subjects who were previously infected with COVID-19<sup>1</sup> and in human subjects who received vaccines against the virus.<sup>2</sup> This technology, GC-FP, has also been leveraged for a highly multiplexed diagnostic assay for Lyme disease in humans, based on detection of antibodies against up to 16 different

antigens of the causative agent, *Borrelia burgdorferi*.<sup>3,4</sup> While antibody-based serological assays are important for monitoring past infections or response to vaccination, the goal of this work was to extend GC-FP technology to direct detection of SARS-CoV-2 antigens, to demonstrate its potential as an acute disease diagnostic versus a purely serological test.

To date, there have been a plethora of emergent approaches for SARS-CoV-2 detection and diagnosis. Several comprehensive reviews have recently been published that cover the full range of both new technologies and legacy diagnostic technologies that have been brought to bear during the pandemic.<sup>5–9</sup> For direct detection of infection, the most common approaches are nucleic acid-based tests, such as reverse transcription polymerase chain reaction (RT-PCR) (for viral genome detection) and easy to use lateral flow-based tests

that detect viral antigens. For most PCR-based approaches, testing requires established laboratory facilities and well-trained personnel, while taking multiple hours to obtain a result. This is in stark contrast to lateral flow tests which can be performed outside of the laboratory by unskilled personnel, including the test subject, in 15–20 min. Serological testing follows a similar pattern, with more complicated laboratory-based tests such as the enzyme-linked immunosorbent assay (ELISA) and microsphere immunoassays (e.g. Luminex) versus lateral flow-based tests targeted to antibody detection. Similar to direct viral detection approaches, the laboratory-based ELISA and microsphere immunoassay tests take multiple hours to complete, while lateral flow-based tests can be performed in minutes.

New approaches to direct detection of SARS-CoV-2 virus particles or antigens include bioelectronic and electrochemical methods, nanopore sensors, and integrated photonic sensors, among others. For serological testing, a number of optical-based approaches have come to the forefront. These include our recent demonstration of the GC-FP technology, surface plasmon resonance imaging (SPRi),<sup>10</sup> and integrated silicon photonic biosensors.<sup>11,12</sup> While Cognetti and Miller<sup>11</sup> have demonstrated both antibody and antigen detection on the same platform, we are unaware of other novel biosensor platforms that have demonstrated this dual mode of detection. Thus, in this work we explored the possibility of detecting SARS-CoV-2 antigens (as a marker of acute disease) and anti-SARS-CoV-2 antibodies (produced as a response to infection or vaccination). We also measured the limits of detection (LoD) for both the antigen and antibody tests. Clinically, such a platform could provide unique information about a subject's infection or vaccination history while at the same time assessing their disease status. This dual-mode detection approach could also help to assess the level of viral antigen present in the blood post-vaccination, in conjunction with antibodies being produced in response to that same vaccination.

## Materials and methods

Nucleocapsid (Nuc) protein, the S1 fragment of the spike protein (S1), the extracellular domain of the spike protein (S1S2), human serum albumin (HSA), MM05 monoclonal mouse anti-Nuc antibody (MM05), MM08 monoclonal mouse anti-Nuc antibody (MM08), R019 monoclonal rabbit anti-Nuc antibody (R019), and R004 monoclonal rabbit anti-Nuc antibody (R004) were all obtained from Sino Biological (Wayne, PA), Inc. Negative control protein, human IgG protein (Hum IgG), SuperBlock blocking buffer, and phosphate-buffered saline (PBS) were obtained from ThermoFisher Scientific (Waltham, MA). PBS-TWEEN (PBS-T) solution consisting of PBS + 0.05% v/v TWEEN-20 (Sigma-Aldrich, St. Louis, MO) was prepared for all experiments. AlexaFluor 647 labeled anti-human IgG (heavy and light chain), anti-rabbit IgG (heavy and light chain), and anti-mouse IgG (heavy and light chain) were obtained from Invitrogen/ThermoFisher Scientific (Waltham, MA).

Gold-coated GC-FP biosensor chips were fabricated as described previously.<sup>3,4</sup> GC-FP chips were printed with an array of 400- $\mu$ m diameter spots of target and control antigens/proteins using an ArrayIt SpotBot II microarray

printer. Proteins/antigens were first diluted to 500  $\mu$ g/mL in PBS and then further diluted 1:1 just prior to printing with GBL protein array printing buffer (Grace Bio-Labs, Bend, OR). For printing, a 180- $\mu$ m diameter printing tip was used, at a relative humidity of 60–70%, at ambient temperature (~25 °C). After printing, chips were allowed to dry at ambient temperature (~25 °C) for 30 min and were then transferred to a sealed container with desiccant for long-term storage (up to 4 weeks) before use.

Blood samples were obtained from COVID-19 positive individuals as well as individuals who tested negative for COVID-19, and individuals who had received a vaccine against COVID-19. Blood sampling was performed under approval of the SUNY Polytechnic Institute Institutional Review Board (protocol #IRB-2020-10).

Two versions of the GC-FP diagnostic chip were developed to directly detect the SARS-CoV-2 Nuc protein, as shown in Figure 1. The first layout, referred to as V21, utilized both R019 anti-Nuc and MM05 anti-Nuc monoclonal antibodies as capture antibodies, with additional positive controls (SARS-CoV-2 Nuc protein) and negative controls (human IgG, SARS-CoV-2 S1/S2 protein, and HSA). After initial studies using V21 chips, additional capture antibodies were added to generate chip version V22. For V22, R004 and MM08 anti-Nuc monoclonal antibodies were added, based on a study that evaluated various antibody pairs for direct detection of SARS-CoV-2 Nuc protein.<sup>13</sup>

The direct detection GC-FP chip processing procedure is outlined in Figure 2. Prior to performing GC-FP detection assays, GC-FP chips were filled with SuperBlock blocking buffer, then incubated at room temperature for 15 min. Chips were then placed in a custom fluidic apparatus to provide sequential flow of sample and reagents using the following steps: (1) 500  $\mu$ L of PBS-T at 100  $\mu$ L/min, (2) 500  $\mu$ L of Nuc protein (diluted COVID-19 negative serum) at 30  $\mu$ L/min, (3) 500  $\mu$ L of PBS-T at 100  $\mu$ L/min, (4) 500  $\mu$ L of anti-Nuc antibody at a concentration of 0.25 ng/mL at 100  $\mu$ L/min, (5) 500  $\mu$ L of PBS-T at 100  $\mu$ L/min, (6) 500  $\mu$ L of AlexaFluor 647 tagged antibody (diluted 1:400 in PBS-T) at 100  $\mu$ L/min, and (7) 500  $\mu$ L of PBS-T at 100  $\mu$ L/min. GC-FP chips were then analyzed in a customized Ciencia, Inc. (East Hartford, CT), fluorescent plasmonic imaging instrument. A custom LabView-based software was used to define a region of interest (ROI) for each individual spot on the GC-FP biosensor chip and the fluorescence intensity of each spot was measured. The fluorescence intensity of all spots was normalized to the Hum IgG internal control spots on each chip, to account for variability between individual chips and individual experiments. This process, including the blocking and imaging steps, takes approximately 1 h.

A third GC-FP detection chip was developed (V23) to combine direct SARS-CoV-2 antigen detection and anti-SARS-CoV-2 antibody detection on a single chip. Similar to our previous studies, this chip used four SARS-CoV-2 antigens (Nuc, S1, S1S2, and RBD) for antibody detection,<sup>1,2</sup> along with the R004, MM05, and MM08 antibodies. The second mouse antibody was included as a secondary detection antibody, as there was no conceived disadvantage to its addition. This chip required some additions to the procedure. The chip was run and processed as described above. After that,

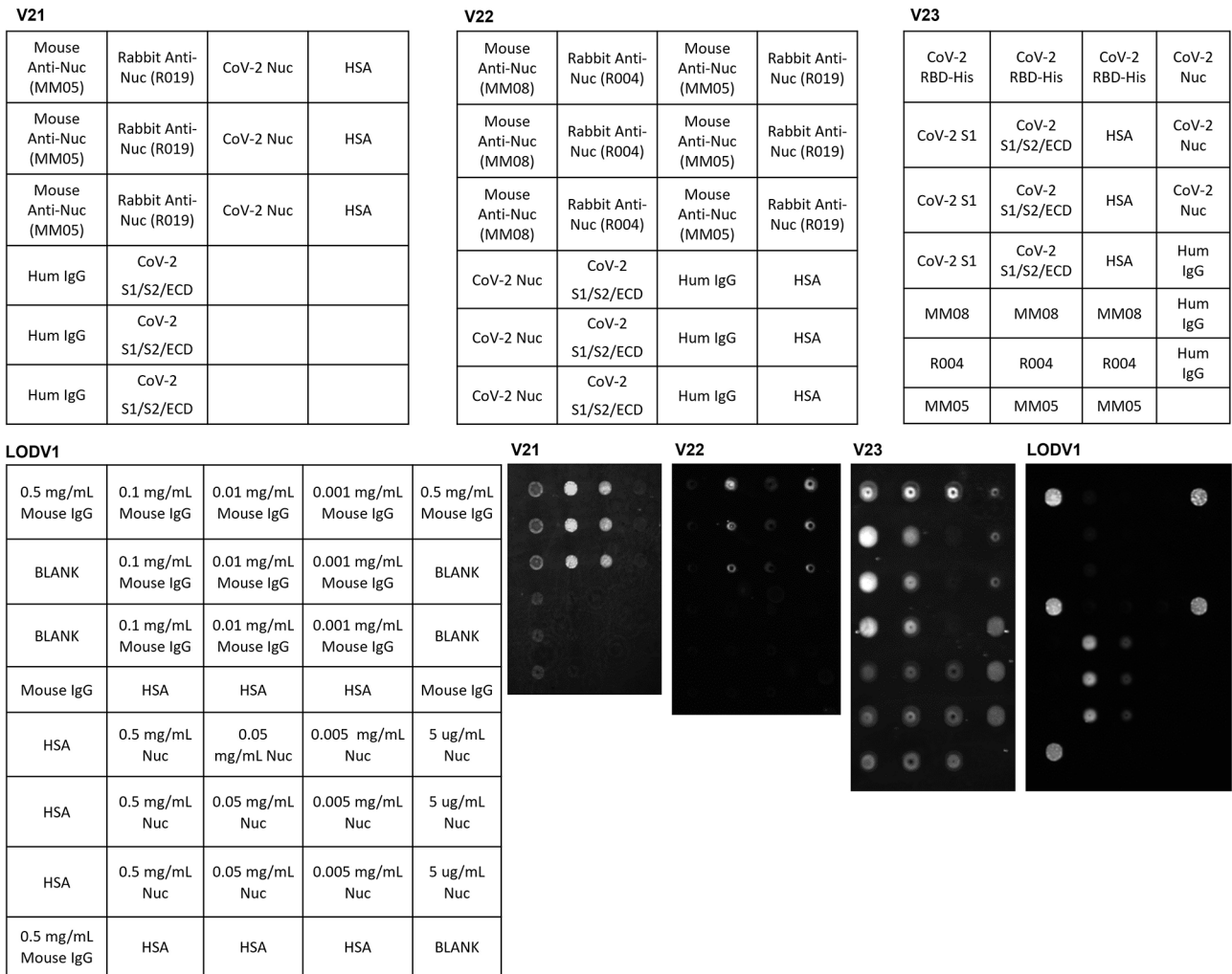


**Figure 1.** Four different versions of a COVID-19 diagnostic GC-FP chip were prepared for this study: V21, V22, V23 and LODV1. The relative position of antibody and antigen spots printed onto each chip are shown in tabular form, while example fluorescent images of each chip are shown in the lower right.

there were two additional run steps. These were (8) 500  $\mu$ L of AlexaFluor 647 tagged anti-human antibody (diluted 1:400 in PBS-T) at 100  $\mu$ L/min and (9) 500  $\mu$ L of PBS-T at 100  $\mu$ L/min. When this was done, the chip was imaged and analyzed a second time. The additional flow steps and imaging step add approximately 15 min to the duration of the assay.

The fourth chip developed in this effort was used to determine the LoD for the previously described antibody detection assay.<sup>1,2</sup> This chip was referred to as LODV1 and its layout can be seen in Figure 1. The proteins used in this assay included an LoD target antigen (Nuc), a positive control (mouse IgG MM08–mIgG), and a negative control (HSA). Nuc was serially diluted in GBL protein array printing buffer to obtain protein (antigen) concentrations of 0.5 mg/mL, 0.05 mg/mL, 0.005 mg/mL, and 0.0005 mg/mL. Similarly, serial dilutions of the positive control mIgG were performed prior to printing, to obtain dilutions of 0.5 mg/mL, 0.1 mg/mL, 0.01 mg/mL, and 0.001 mg/mL. The chips were then printed as described above.

The flow procedure used for LoD experiments was similar to the direct antigen detection procedure. Prior to

microfluidic processing, the LODV1 chips were filled with PBS SuperBlock solution and incubated for 15 min at room temperature. The LODV1 chips were then placed into a custom microfluidic set-up and run through with the reagents in the following manner: (1) 500  $\mu$ L of PBS-T at 100  $\mu$ L/min, (2) 500  $\mu$ L of MM08 sample at 30  $\mu$ L/min, (3) 500  $\mu$ L of PBS-T at 100  $\mu$ L/min, (4) 500  $\mu$ L of AlexaFluor 647 tagged antibody at 100  $\mu$ L/min, and (5) 500  $\mu$ L of PBS-T at 100  $\mu$ L/min. The chips were imaged by the Ciencia, Inc., fluorescent plasmonic imaging instrument and analyzed using the accompanying LabView program. The intensity was again normalized to the Hum IgG internal control spots on each chip, to account for any variability between chips.

Normalized spot intensity data were exported from LabView software and further analyzed using Microsoft Excel and GraphPad Prism 9.0 software (for fitting, receiver operating characteristic analysis, correlation, and statistical analysis). To account for variation between chips and experiments, normalized intensity data for positive control and SARS-CoV-2 antigen spots (mean intensity,  $\bar{x}$ ) were divided by the average negative control spot intensity, plus three

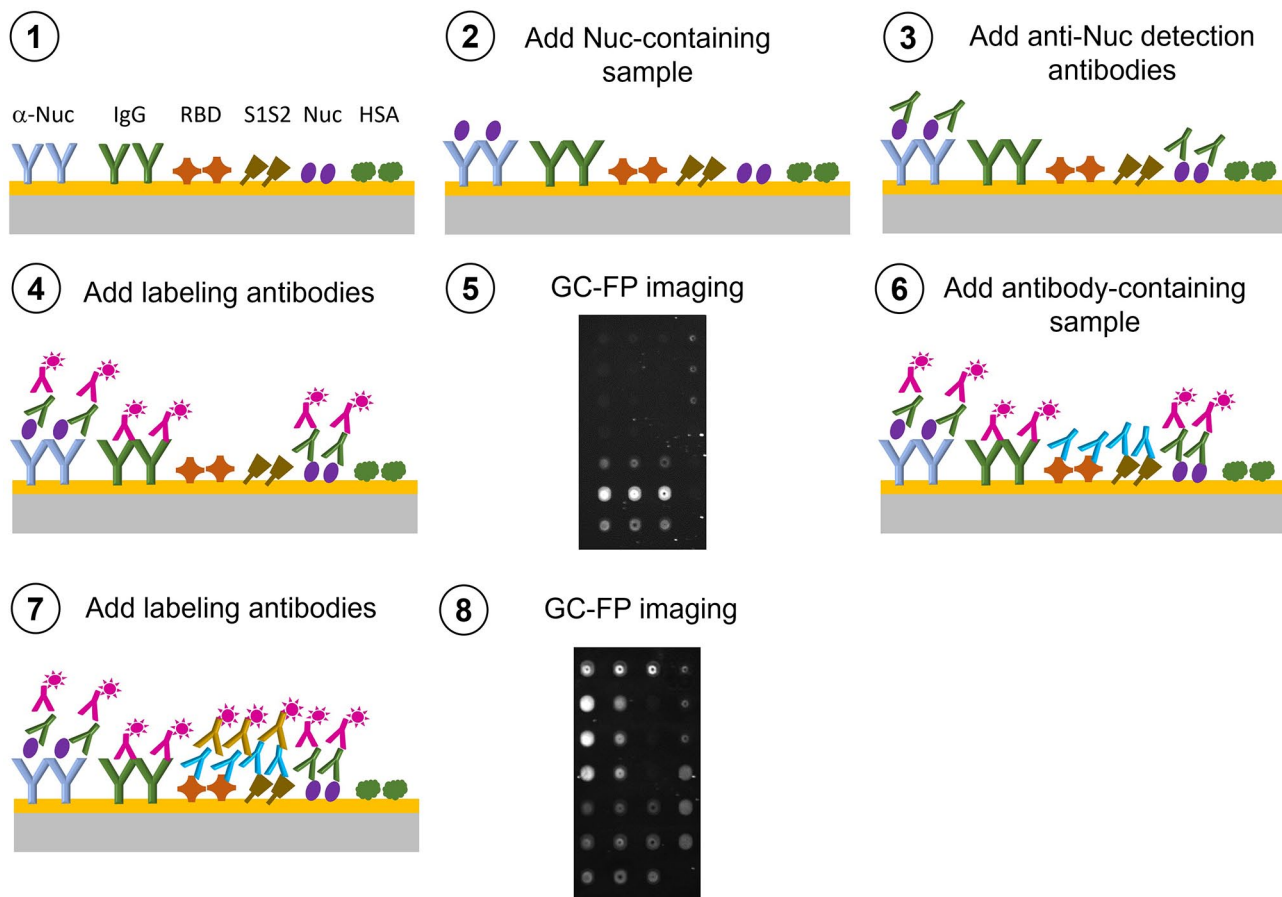


**Figure 2.** General procedure for processing samples on GC-FP chips for both direct antigen detection (steps 1–5) and for additional anti-COVID antibody detection (steps 6–8). (A color version of this figure is available in the online journal.)

times the standard deviation ( $\sigma$ ) of the negative control spot intensity ( $\bar{x} + 3\sigma$ ) to produce a detection metric (detection ratio) as described previously.<sup>1,2</sup>

## Results

Building on our previous demonstration of anti-SARS-CoV-2 antibody detection and Lyme disease diagnosis using GC-FP<sup>1–4</sup> we sought to (1) develop a GC-FP approach for direct antigen detection to be used for COVID-19 diagnosis, (2) quantify the LoD of antibody detection, and then (3) demonstrate combined SARS-CoV-2 antigen and antibody detection on the same GC-FP chip. Two chip designs were explored for direct detection of antigen, V21 and V22 (Figure 1). For the initial study using V21 chips, Nuc antigen and rabbit (R019) antibodies were printed onto GC-FP chips as a positive control while anti-Nuc antibodies R019 and MM05 were evaluated for both capture and detection of Nuc antigen. Conceptually, the goal of the direct detection assay was to capture Nuc antigen with either mouse or rabbit monoclonal antibodies immobilized on the GC-FP chip. Following exposure to sample containing Nuc antigen, the chip would then be labeled with a second monoclonal antibody (from a different host organism than the capture antibody), followed by a second labeling step with an AlexaFluor 647 labeling antibody (see Figure 2). For example, immobilized mouse anti-Nuc monoclonal antibody could be used for capture,

followed by primary labeling with rabbit anti-Nuc monoclonal antibody (detection antibody), and then secondary labeling with AlexaFluor 647 labeled anti-rabbit IgG. In this way, the secondary labeling antibody would only be observed in the presence of both Nuc antigen and the detection antibody (rabbit monoclonal IgG).

Figure 3 shows the results from the first set of experiments with V21 GC-FP chips when Nuc was used at a concentration of 1  $\mu\text{g}/\text{mL}$ . Positive controls and the detection antibody/Nuc/capture antibody complex gave significantly higher GC-FP detection ratios than negative controls. The GC-FP diagnostic ratio for positive controls was much higher ( $\sim 4X$ ) than that measured for the detection antibody/Nuc/capture antibody complex, but this was expected since positive controls consisted of target antigen (Nuc) or the target of our labeling antibody (R019) directly printed onto the GC-FP chip.

After successfully demonstrating proof of concept for direct antigen detection with V21 GC-FP chips, the V22 version was generated to introduce additional capture antibodies for evaluation—MM08 and R004. These were chosen based on a study by Cate *et al.*,<sup>13</sup> which evaluated various pairs of antibodies for direct SARS-CoV-2 antigen detection. As each chip was printed with all four anti-Nuc antibodies (R004, R019, MM05 and MM08), four tests were performed, where a different anti-Nuc antibody was used as the detection antibody in each experiment. For all experiments Nuc

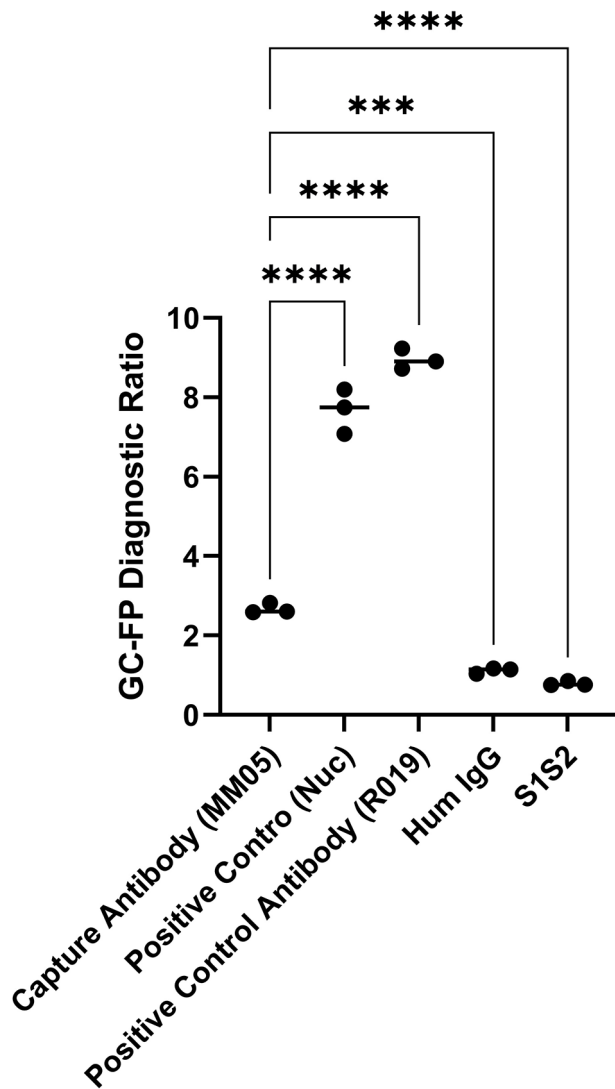


**Figure 3.** GC-FP-based detection of Nuc protein using MM05 as the capture antibody and R019 as the detection antibody. Positive controls included Nuc protein and R019 antibodies directly immobilized on the GC-FP chip. Negative controls included human IgG and CoV-2 S1S2 (spike) protein. One-way ANOVA followed by Tukey's multiple comparison test were performed using these data. \*\*\*  $P=0.0004$ . \*\*\*\*  $P<0.0001$ .

was used at a concentration of 1  $\mu\text{g}/\text{mL}$ . By comparing the GC-FP detection ratio of the different capture antibody spots to the negative controls (S1S2, and Hum IgG), the most significant difference in GC-FP detection ratio was found when using MM05 as the capture antibody and R004 as the detection antibody. The inverse pair (R004 capture / MM05 detection) yielded significant increase in GC-FP detection ratio for the capture antibody/Nuc/detection antibody complex, but less than for the MM05/R004 pair. These results are summarized in Figure 4. The antibody pair of R004 and MM08 also showed potential for direct detection but was not better than the R004/MM05 pair. The results from all possible antibody pairings are summarized in Table 1.

To determine the lower LoD for Nuc using MM05 as the capture antibody and R004 as the detection antibody, a dilution series of Nuc (100 ng/mL–5  $\mu\text{g}/\text{mL}$ ) mixed with a 1:100 dilution of human serum negative for COVID-19

was generated and individual dilutions were run on separate V22 GC-FP chips. As seen in Figure 5, concentrations of Nuc below 1  $\mu\text{g}/\text{mL}$  yielded GC-FP detection ratios in the range of 1–1.4. The GC-FP detection ratio compares the fluorescence intensity from a test spot to the mean intensity (+3 standard deviations) of a negative control spot (in this case, human serum albumin, HSA). Thus, using conventional definitions of LoD (mean background intensity + 3 standard deviations), any GC-FP detection ratio value above 1.0 technically represents a measurable signal. Given the data presented in Figure 5, however, we are not confident in this approach and therefore assign the LoD for Nuc as 1  $\mu\text{g}/\text{mL}$  or higher. This limit may be improved by using other detection antibodies.

For optimization of the GC-FP antibody detection technology, an additional chip (LODV1) was developed to establish a range of sample concentrations where the biosensor could effectively detect antibody binding. This chip was also designed to test the effect of the concentration of printed antigens on antibody detection levels, which in this case was the Nuc antigen. Our previous work on GC-FP utilized a 0.5 mg/mL concentration for antigen and printing buffer. To find the optimal concentration of antigen in printing buffer, target antigen Nuc was printed in varying dilutions from 500  $\mu\text{g}/\text{mL}$  to 0.5 mg/mL. Positive control mIgG spots were printed in concentrations ranging from 0.1 to 0.001 mg/mL and HSA was used as a negative control, printed at 0.5 mg/mL. To determine optimal antigen concentration on spots and the LoD for antibody targets, MM08 was used, diluted with PBS-T from 0.01 mg/mL to 10 ng/mL. Experimental data demonstrated that the best Nuc antigen concentration for spotting on chips was 0.5 mg/mL, as lower dilutions showed negligible differences in positive signal for different concentrations of antibody. Figure 6 shows the GC-FP detection ratio measured for each concentration of MM08 that was used, with a non-linear regression fit of the data, assuming binding kinetics to saturation (GraphPad Prism 9.0). The GC-FP diagnostic ratio remained above 1.0 down to a concentration of 25 ng/mL (GC-FP detection ratio = 1.22). At the next higher concentration (50 ng/mL) the GC-FP detection ratio rose to 3.46. As described previously, the GC-FP detection ratio accounts for the background signal and noise and thus the true LoD may be as low as 25 ng/mL. For a higher confidence measure of the LoD, however, we propose 50 ng/mL, which represents a significant increase in GC-FP detection ratio from the minimum value of 1.0.

A final version of the GC-FP chip, V23, was developed for a combination of direct antigen and antibody detection. This design combined the direct antigen detection assay described above with the previously described antibody detection assay.<sup>1,2</sup> For direct detection of Nuc, MM05 served as the capture antibody with R004 as the detection antibody, while MM08 was included as a potential alternative capture antibody and R004 was included as a positive control (Figure 1). For the SARS-CoV-2 antibody detection component of the V23 chip, the same antigens were used as previous work (S1, S1S2, RBD, Nuc). Multiple other negative and positive controls were also included, and HSA was used as the overall negative control and for determination of the GC-FP detection ratio.

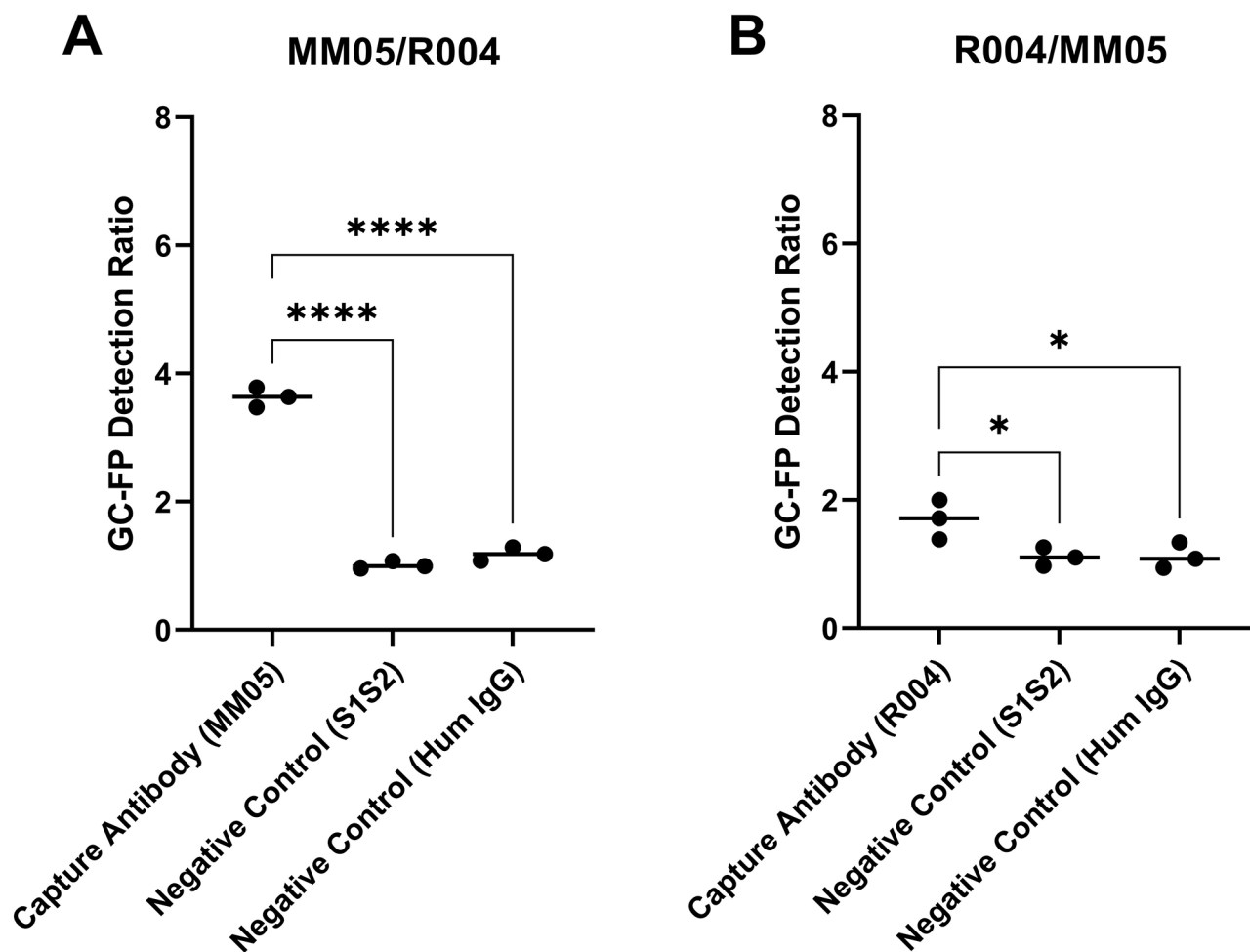


**Figure 4.** Direct SARS-CoV-2 Nuc antigen detection via GC-FP for the capture/detection antibody pairs of MM05/R004 and R004/MM05. One-way ANOVA and Tukey's multiple comparison test showed significant differences between the capture/detection antibody pairs and negative controls. \* $P < 0.05$ . \*\*\*\* $P < 0.0001$ .

**Table 1.** Evaluation of capture and detection antibody pairs on V22 chips for direct detection of CoV-2 Nuc protein.

Capture antibody	Detection antibody	Mean GC-FP detection ratio (3 spots)		
		Negative control (S1S2)	Negative control (human IgG)	Anti-Nuc antibody
MM08	R004	1.01	1.19	1.89**
MM05	R004	1.01	1.19	3.63****
MM08	R019	1.01	1.07	1.42
MM05	R019	1.01	1.07	1.35
R004	MM05	1.11	1.12	1.70**
R019	MM05	1.11	1.12	1.47
R004	MM08	0.98	1.33	1.58*
R019	MM08	0.98	1.33	1.72

The capture and detection antibody are listed for each pair, along with the GC-FP detection ratio for two different sets of negative control spots (CoV-2 S1S2 and human IgG) and the GC-FP detection ratio for the capture/detection antibody spots. One-way ANOVA followed by Tukey's multiple comparison test yielded significant difference in GC-FP ratio for three of the antibody pairs (\*\* $P < 0.05$ , \*\*\*\* $P < 0.0001$ ). (\*For R004/M008 antibody GC-FP ratio was only significantly different from S1S2, and not significantly different ( $P > 0.05$ ) from human IgG). GC-FP: grating coupled fluorescent plasmonic.

For dual detection experiments, a sample of human blood serum was used, from a subject who was confirmed by PCR to be COVID-19 positive (2 weeks post infection). Thus, the sample was expected to have high levels of antibodies against SARS-CoV-2 antigens, but would likely have a very low concentration of Nuc antigen, due to the fact that the

subject had recovered from COVID-19 for a full 2 weeks. Thus, this sample was first diluted 1:100 in PBS-T buffer and then Nuc antigen was added to yield a final concentration of 1  $\mu\text{g}/\text{mL}$ . A V23 chip was then used for the experiment, using the step-by-step protocol outlined in Figure 2. Briefly, the sample was applied to the chip, followed by addition of

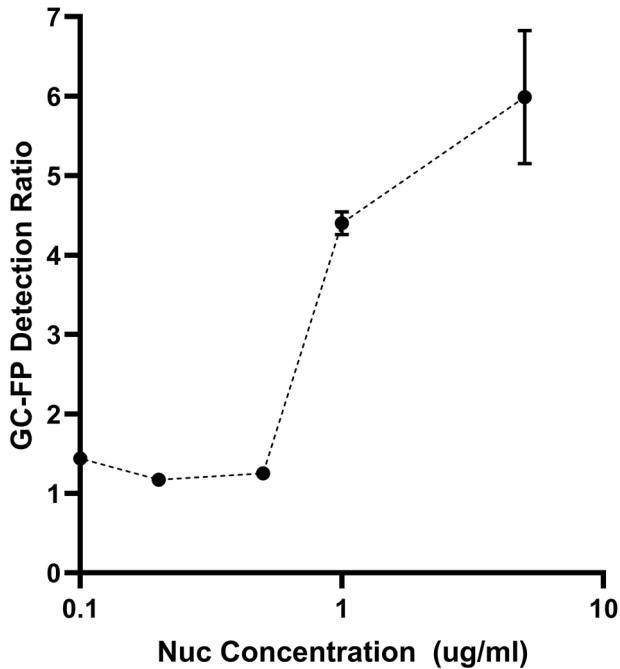


**Figure 5.** Direct CoV-2 Nuc antigen detection via GC-FP as a function of Nuc concentration. Error bars represent one standard deviation in GC-FP detection ratio, for three replicate spots.

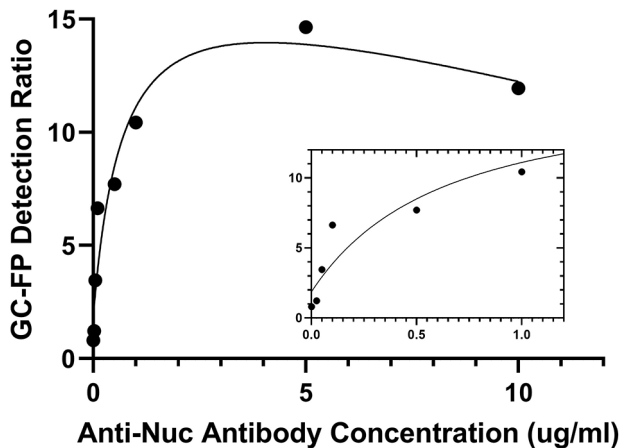


**Figure 6.** GC-FP detection ratio as a function of anti-Nuc antibody concentration. MM08 anti-Nuc antibodies were applied to LODV1 chips in a range of 1 ng/mL–10  $\mu$ g/mL. Non-linear regression using a binding model with saturation was used to fit the data, yielding an  $R$ -square of 0.9315.

the detection antibody (R004) and AlexaFluor 647 anti-rabbit labeling antibody. After GC-FP imaging, AlexaFluor 647 anti-human IgG was added to recognize the anti-SARS-CoV-2 antibodies present in the sample, followed by washing and GC-FP imaging. The combined results of this experiment are shown in Figure 7. Detection of Nuc antigen was low, but significantly ( $P < 0.05$ ) above negative controls (Figure 7A). Detection of antibodies was also significant ( $P < 0.0001$ ) for all SARS-CoV-2 spike protein antigens (RBD, S1, and S1S2). Antibodies against Nuc antigen were well above the GC-FP detection ratio baseline of 1.0, but this increase was not

found to be statistically significant. This may be due to lower levels of anti-Nuc antibodies in this particular subject (post infection) or could have resulted from anti-Nuc antibodies in the sample binding to the Nuc antigen that we added to the solution. In this scenario, anti-Nuc antibodies may have been present, but were titrated away from the Nuc spots on the chip by the free Nuc protein in solution.

## Discussion

There is a continuing need for biosensors that are capable of diagnosing COVID-19 disease and for detecting an immune response to COVID-19 infection, typically by measuring antibody levels in blood, plasma, or serum. In this work, we have shown the potential for using a single chip-based biosensor platform (GC-FP) to sequentially detect SARS-CoV-2 Nuc antigen and then anti-SARS-CoV-2 antibodies in the same sample. The entire test takes 1 h and is performed with a small volume of sample (approximately 5  $\mu$ L of serum diluted 1:100 in PBS-T).

To date, we are only aware of one other biosensor platform that can perform similar detection of both antibody and antigen, which is an integrated silicon photonics platform described by Cognetti and Miller<sup>11</sup> In this work, Nuc protein was the SARS-CoV-2 antigen target and the threshold for detection was approximately 10  $\mu$ g/mL, as compared to the 1  $\mu$ g/mL LoD for our GC-FP detection approach. Furthermore, the work by Cognetti *et al.* utilized two separate photonic chips, one for antigen detection and another for antibody detection, and therefore requires additional handling steps and consumables (chips) to achieve the same result that we obtain with a single GC-FP chip. ELISA-based approaches should also be amenable to detection of both antibodies and antigens, but separate ELISA wells must be used for each target, and the entire detection process requires significantly more time (~4 h) and typically requires a larger volume of washing and labeling reagents. Thus, our GC-FP-based approach offers the simplest approach to date for dual detection of antibody and antigen from a single sample, using a single biosensor consumable (chip).

The LoD for antigen detection that we have determined with our GC-FP detection approach (1  $\mu$ g/mL) is relatively high compared with the expected concentrations in blood samples from COVID-19 positive subjects. Several studies have assessed the concentration of Nuc antigen in blood serum from infected individuals. These concentrations range from ~100 pg/mL to a maximum of 100,000 pg/mL (100 ng/mL)<sup>14,15</sup> and are well below our LoD of 1  $\mu$ g/mL. This suggests that our GC-FP-based approach may not be appropriate for detection of Nuc antigen in blood; however, higher concentrations of Nuc can be found in nasopharyngeal swabs (ranging from 100 pg/mL to  $\gg 100$   $\mu$ g/mL),<sup>16</sup> which makes this sample matrix a potential target for future work on direct antigen detection with GC-FP.

The initial antibody detection data from this study is consistent with our previous work and demonstrates that the additional antigen detection step does not significantly alter detection of antibodies against SARS-CoV-2 spike antigens. As seen in Figure 7, the anti-Nuc antibody levels are not

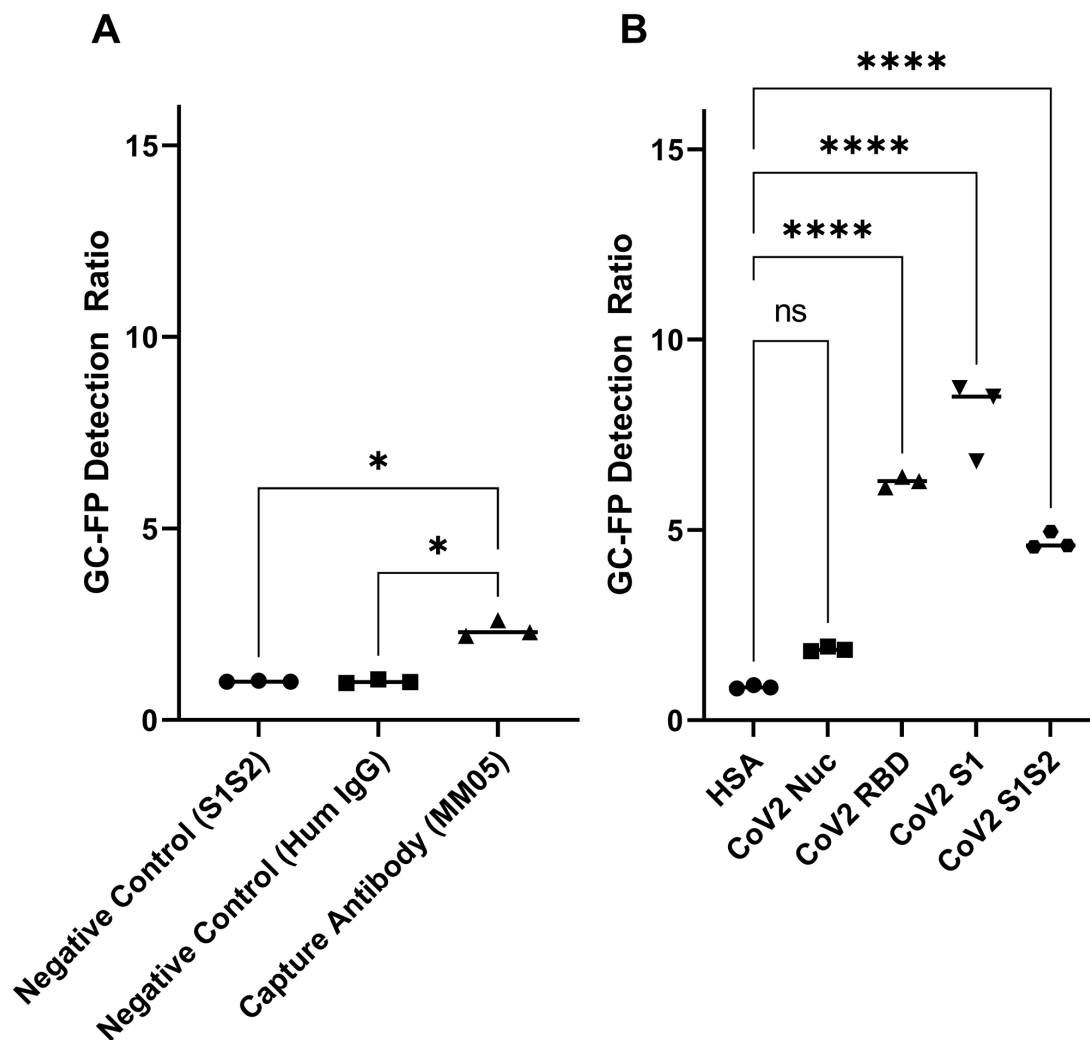


**Figure 7.** Direct detection of SARS-CoV-2 Nuc antigen (A) and subsequent detection of anti-SARS-CoV-2 antibodies (B) from a confirmed COVID-19 positive human serum sample.

CoV-2 Nuc antigen was added to the sample 1  $\mu\text{g}/\text{mL}$  concentration. One-way ANOVA and Tukey's multiple comparison test were performed following calculation of the GC-FP detection ratio for each set of spots.

\*  $P < 0.05$ . \*\*\*\*  $P < 0.0001$ .

statistically different than the negative control (HSA). This may be due to low anti-Nuc antibody levels in this particular subject, but could also be due to interference between the soluble Nuc protein added to the sample (for antigen detection) and any anti-Nuc antibodies in the sample. Additional work will be needed to explore this possibility, using the large cohort of blood/serum samples that we have collected for prior efforts.<sup>1,2</sup>

In summary, we have demonstrated GC-FP-based detection of both SARS-CoV-2 Nuc antigen and anti-SARS-CoV-2 antibodies from a single sample using a single consumable detection chip. With a total assay time of 1 h, this represents a significant improvement over performing separate tests on different platforms and raises the potential for combined antibody/antigen testing for diagnostic purposes. Additional optimization will be needed to reduce the LoD for antigens and to determine the diagnostic power of this approach using a larger set of human blood/serum samples.

#### AUTHORS' CONTRIBUTIONS

BT and AG performed experiments, data collection, analysis, and contributed to writing of the article. NCC was involved in experimental design, data analysis, writing, and review of the article.

#### ACKNOWLEDGEMENTS

The authors acknowledge instrumentation and software support from Ciencia, Inc.

#### DECLARATION OF CONFLICTING INTERESTS

The author(s) declared no potential conflicts of interest with respect to the research, authorship, and/or publication of this article.


#### FUNDING

The author(s) disclosed receipt of the following financial support for the research, authorship, and/or publication of this article:



This work was supported in part by the Center of Advanced Technology (CATN2) at SUNY Polytechnic Institute and the SUNY COVID-19 seed funding program.

#### ORCID ID

Nathaniel C Cady  <https://orcid.org/0000-0003-4345-3627>

#### REFERENCES

- Cady NC, Tokranova N, Minor A, Nikvand N, Strle K, Lee WT, Page W, Guignon E, Pilar A, Gibson GN. Multiplexed detection and quantification of human antibody response to COVID-19 infection using a plasmon enhanced biosensor platform. *Biosens Bioelectron* 2021;**171**:112679
- Taubner B, Peredo-Wende R, Ramani A, Singh G, Strle K, Cady NC. Rapid and quantitative detection of human antibodies against the 2019 novel coronavirus SARS CoV2 and its variants as a result of vaccination and infection. *Microbiol Spectr* 2021;**9**:e0089021
- Chou E, Lasek-Nesselquist E, Taubner B, Pilar A, Guignon E, Page W, Lin YP, Cady NC. A fluorescent plasmonic biochip assay for multiplex screening of diagnostic serum antibody targets in human Lyme disease. *PLoS ONE* 2020;**15**:e0228772
- Chou E, Pilar A, Guignon E, Page W, Lin Y-P, Cady N. Rapid and multiplexed detection of Lyme disease using a grating coupled-fluorescent plasmonics (GC-FP) biosensor platform. *SPIE Bios* 2019;**10895**:108950C
- Fathi Karkan S, Maleki Baladi R, Shahgolzari M, Gholizadeh M, Shayegh F, Arashkia A. The evolving direct and indirect platforms for the detection of SARS-CoV-2. *J Virol Methods* 2022;**300**:114381
- Flores-Contreras EA, Gonzalez-Gonzalez RB, Rodriguez-Sanchez IP, Yee-de Leon JF, Iqbal HMN, Gonzalez-Gonzalez E. Microfluidics-based biosensing platforms: emerging frontiers in point-of-care testing SARS-CoV-2 and seroprevalence. *Biosensors (Basel)* 2022;**12**:179
- Ilkhani H, Hedayat N, Farhad S. Novel approaches for rapid detection of COVID-19 during the pandemic: a review. *Anal Biochem* 2021;**634**:114362
- Safiabadi Tali SH, LeBlanc JJ, Sadiq Z, Oyewunmi OD, Camargo C, Nikpour B, Armanfard N, Sagan SM, Jahanshahi-Anbuhi S. Tools and techniques for severe acute respiratory syndrome coronavirus 2 (SARS-CoV-2)/COVID-19 detection. *Clin Microbiol Rev* 2021;**34**:e00228–20
- Taha BA, Al Mashhadany Y, Bachok NN, Ashrif ABA, Hafiz Mokhtar MH, Dzulkefly Bin Zan MS, Arsad N. Detection of COVID-19 virus on surfaces using photonics: challenges and perspectives. *Diagnostics (Basel)* 2021;**11**:1119
- Steglich P, Schasfoort RBM. Surface plasmon resonance imaging (SPRI) and photonic integrated circuits (PIC) for COVID-19 severity monitoring. *COVID* 2022;**2**:389–97
- Cognetti JS, Miller BL. Monitoring serum spike protein with disposable photonic biosensors following SARS-CoV-2 vaccination. *Sensors (Basel)* 2021;**21**:5857
- Cognetti JS, Steiner DJ, Abedin M, Bryan MR, Shanahan C, Tokranova N, Young E, Klose AM, Zavriyev A, Judy N, Piorek B, Meinhart C, Jakubowicz R, Warren H, Cady NC, Miller BL. Disposable photonics for cost-effective clinical bioassays: application to COVID-19 antibody testing. *Lab Chip* 2021;**21**:2913–21
- Cate DM, Bishop JD, Hsieh HV, Glukhova VA, Alonzo LF, Hermansky HG, Barrios-Lopez B, Grant BD, Anderson CE, Spencer E, Kuhn S, Gallagher R, Rivera R, Bennett C, Byrnes SA, Connelly JT, Dewan PK, Boyle DS, Weigl BH, Nichols KP. Antibody screening results for anti-nucleocapsid antibodies toward the development of a lateral flow assay to detect SARS-CoV-2 nucleocapsid protein. *ACS Omega* 2021;**6**:25116–23
- Hingrat QL, Visseaux B, Laouenan C, Tubiana S, Bouadma L, Yazdanpanah Y, Duval X, Burdet C, Ichou H, Damond F, Bertine M, Benmalek N, Choquet C, Timsit JF, Ghosn J, Charpentier C, Descamps D, Houhou-Fidouh N, French COVID Cohort Management Committee, CoV-CONTACT Study Group. Detection of SARS-CoV-2 N-antigen in blood during acute COVID-19 provides a sensitive new marker and new testing alternatives. *Clin Microbiol Infect* 2020;**27**:789.e1–e5
- Zhang Y, Ong CM, Yun C, Mo W, Whitman JD, Lynch KL, Wu AHB. Diagnostic value of nucleocapsid protein in blood for SARS-CoV-2 infection. *Clin Chem* 2021;**68**:240–8
- Pollock NR, Savage TJ, Wardell H, Lee RA, Mathew A, Stengelin M, Sigal GB. Correlation of SARS-CoV-2 nucleocapsid antigen and RNA concentrations in nasopharyngeal samples from children and adults using an ultrasensitive and quantitative antigen assay. *J Clin Microbiol* 2021;**59**:e03077–20

(Received April 8, 2022, Accepted June 21, 2022)